Samm50 Promotes Hypertrophy by Regulating Pink1-Dependent Mitophagy Signaling in Neonatal Cardiomyocytes

Ran Xu[†], Le Kang[†], Siang Wei, Chunjie Yang, Yuanfeng Fu, Zhiwen Ding* and Yunzeng Zou*

Shanghai Institute of Cardiovascular Diseases, Zhongshan Hospital, Fudan University, Shanghai, China

Pathological cardiac hypertrophy, the adaptive response of the myocardium to various pathological stimuli, is one of the primary predictors and predisposing factors of heart failure. However, its molecular mechanisms underlying pathogenesis remain poorly understood. Here, we studied the function of Samm50 in mitophagy during Ang II-induced cardiomyocyte hypertrophy via lentiviruses mediated knockdown and overexpression of Samm50 protein. We first found that Samm50 is a key positive regulator of cardiac hypertrophy, for western blot and real-time quantitative PCR detection revealed Samm50 was downregulated both in pressure-overload-induced hypertrophic hearts and Ang II-induced cardiomyocyte hypertrophy. Then, Samm50 overexpression exhibits enhanced induction of cardiac hypertrophy marker genes and cell enlargement in primary mouse cardiomyocytes by qPCR and immunofluorescence analysis, respectively. Meanwhile, Samm50 remarkably reduced Ang II-induced autophagy as indicated by decreased mitophagy protein levels and autophagic flux, whereas the opposite phenotype was observed in Samm50 knockdown cardiomyocytes. However, the protective role of Samm50 deficiency against cardiac hypertrophy was abolished by inhibiting mitophagy through Vps34 inhibitor or Pink1 knockdown. Moreover, we further demonstrated that Samm50 interacted with Pink1 and stimulated the accumulation of Parkin on mitochondria to initiate mitophagy by co-immunoprecipitation analysis and immunofluorescence. Thus, these results suggest that Samm50 regulates Pink1-Parkin-mediated mitophagy to promote cardiac hypertrophy, and targeting mitophagy may provide new insights into the treatment of cardiac hypertrophy.

Keywords: cardiac hypertrophy, mitophagy, Samm50, Pink1, heart failure

INTRODUCTION

Heart failure, a complex multifactorial syndrome, has now become a worldwide problem reaching epidemic proportions. Cardiac hypertrophy is regarded as the leading cause of heart failure. The onset of cardiac hypertrophy is characterized by a fetal reprogramming of gene expression where adult genes are repressed and fetal genes are activated, resulting in an imbalance between protein synthesis and degradation (1–3). At the molecular level, pathological hypertrophy has been

associated with mitogen-activated protein kinase signaling pathways, insulin-like growth factor-I phosphatidylinositol 3-kinase (PI3K)-AKT/protein kinase B mammalian target of rapamycin (mTOR) signaling pathways, calcium signaling pathway, chromatin remodeling and so on (4–8). Although considerable progress has been made in elucidating the molecular mechanism of cardiac hypertrophy, there remain many unknowns.

Over the last decade, many studies have demonstrated that autophagy participates in the pathogenesis of cardiac hypertrophy. For example, cardiac-specific deficiency of Atg5 mice with pressure overload developed cardiac dysfunction and left ventricular dilatation (9). Furthermore, the key inhibitor of the mTOR pathway rapamycin, which is a potent activator of autophagy, has been reported to prevent cardiac hypertrophy (10, 11). Mitophagy, a special autophagy, removes damaged or redundant mitochondria to maintain heart function in response to various stress and heart disease conditions. PTEN-induced kinase1 (Pink1) is a key molecule for mediating mitophagy. Basally, Pink1 is rapidly degraded when it is translocated into mitochondria. However, in any case, if Pink1 is accumulated in the outer membrane of mitochondria (OMM), it would phosphorylate Parkin leading to activating its ligase activity. OMM proteins would be ubiquitinated, and autophagic receptors are recruited. A series of events eventually lead to the mitochondria being delivered to lysosomes (12–18).

All nuclear DNA-encoded mitochondrial proteins must be transported into mitochondria through channels in the OMM. The channel-forming protein Tom40 and voltage-dependent anion channel proteins (VDACs) play key roles (19). The sorting and assembly machinery (SAM) is critical for membrane integration and assembly of Tom40 and VDACs into the mitochondrial outer membrane. SAMM50 sorting and assembly machinery component (Samm50), a member of the SAM complex, contains a β-barrel domain that is conserved in evolution from bacteria to humans (20, 21). Samm50 is considered to be an essential protein present on the outer mitochondrial membrane, and it has been confirmed that it promotes the biogenesis of ß-barrel protein by directly interacting with the TOM complex. Samm50 interact with core proteins of the mitochondrial contact site and cristae organizing system complex to regulate cristae stability (22). Long-term lack of Samm50 influences the protein quantity of all large respiratory complexes of mitochondrial coding subunits, as well as mitochondrial swollen and mitochondrial inheritance impaired (23, 24). Samm50 also plays a key role in regulating Pink1 degraded through direct interaction (25).

Although Samm50 is a key regulatory factor of Pink1 and might affect mitophagy, whether it regulate the Pink1-Parkin pathway and involve in cardiac hypertrophy remains poorly understood. In this study, we found that Samm50 was downregulated in the cardiac hypertrophy model. Samm50 knockdown or overexpression was confirmed to mitigate or aggravate Angiotensin II (Ang II) induced cardiomyocyte hypertrophy, respectively. Mechanistically, we found that Samm50 inhibit mitophagy through interacting with Pink1.

Collectively, we propose that Samm50 regulates mitophagy in cardiomyocytes and mediates pathological hypertrophy.

MATERIALS AND METHODS

Cell Culture and Treatment

Mouse neonatal ventricular cardiomyocytes were separated from 1–2-day-old neonatal C57BL/6J mice using enzymatic dissociation and cultured as previously described (26). Briefly, neonatal mice hearts were cut into small pieces and digested in 0.125 mg/ml trypsin (Gibco, #15090046) at 37°C. Then the supernatant was collected with complete Dulbecco's modified Eagle medium: Nutrient Mixture F-12 (DMEM/F12, Gibco, #8120319) and centrifuged at 600 g for 5 min. After repeating this cycle 6–8 times, the cell pellets were resuspended in DMEM/F12 containing 10% fetal bovine serum (FBS, Gibico, #10099133C), passed through a 100 mm cell strainer, and plated onto 10 cm dishes for 1.5 h at 37°C in 5% CO_2. The supernatant was then obtained and plated on dishes for further experiments. For gene overexpression and knockdown studies, cardiomyocytes were infected with lentiviruses according to the manufacturer's protocol. Recombinant lentiviruses were designed and synthesized by Fubio Biological Technology. After lentiviral transduction for 72–96 h, cardiomyocytes were stimulated with 10^{-6} M Ang II (Sigma, #A9525) for the indicated time points.

HL-1 cardiac muscle cell line (HL-1 cell) was purchased from Sigma-Aldrich (#SCC065) and maintained in Claycomb medium (Sigma-Aldrich, #51800C) supplemented with 10% FBS and 2 mM L-glutamine. Plasmids were transfected according to the manufacturer's protocol. After starving for 24 h in serum-free Claycomb medium, the cells were treated with 10^{-6} M Ang II for 24 h and followed by co-immunoprecipitation (co-IP) experiments.

Plasmids and Reagents

Pink1-Flag and Samm50-influenza hemagglutinin (HA) complementary DNA (cDNA) were cloned into the pcDNA3.1 vector. Short hairpin RNA (shRNA) against Samm50 and Pink1 were performed using the pLKO vector. The target sequences of shRNA oligonucleotides were listed in **Supplementary Table 1**. The Vps34 inhibitor was purchased from MCE (#HY-12794). Lipo8000 transfection reagent was purchased from Beyotime (#C0533).

Transverse Aortic Constriction Model

C57BL/6J male mice (10–12 weeks) were subjected to transverse aortic constriction (TAC) to simulate the pressure overload model, and mice were sacrificed two weeks after surgery. After opening the chest cavity and separating the aortic arch, a 27-gauge needle was placed on the aorta between the left common carotid artery and the innominate artery, followed by ligation with 6-0 silk. Then, the needle was removed to generate aortic constriction. The Sham group mice underwent an identical surgery apart from the ligation. The animal study was reviewed and approved by the Animal Care and Use Committee of Zhongshan Hospital, Fudan University.

RNA Isolation and Quantitative PCR Analysis

Total RNA was extracted with the TRIzol reagent (Ambion, #257401). cDNA was generated using PrimeScript^{TM} RT Reagent Kit with gDNA Eraser (Takara, #RR047A) following the manufacturer's instructions. Quantitative real-time polymerase chain reaction (qRT-PCR) was performed by ChamQ Universal SYBR qPCR Master Mix (Vazyme, #Q711-02) on a Bio-Rad IQ5 multicolor detection system. The program was as follows: 5 min at 95°C followed by 40 cycles of 20 s at 95°C and 30 s at 60°C. The results were analyzed using the $2^{-\Delta\Delta Ct}$ method [27]. The primer sequences were listed in **Supplementary Table 2**.

Immunoblot and Co-immunoprecipitation Assay

Proteins were obtained from tissues and cells lysed in lysis buffer (Beyotime, #P0013B). Then, samples were separated by 10–15% SDS-polyacrylamide electrophoresis gel and transferred to PVDF membranes. After blocking in 5% BSA, blots were incubated with the primary antibodies at 4°C overnight, followed by incubation with peroxidase-conjugated rabbit secondary antibody (Thermo Fisher, #A0545, 1:5000) at room temperature for 1 h. The following antibodies were used in this study: anti-GAPDH (Proteintech, #HRP-60004, 1:10000), anti-LC3 (Cell Signaling Technology, #2775, 1:1000), anti-COX4 (Proteintech, #11242-1-AP, 1:1000), anti-Pink1 (Proteintech, #23274-1-AP, 1:1000), anti-Parkin (Proteintech, #14060-1-AP, 1:1000), anti-Samm50 (Abcam, #ab133709, 1:5000) and anti-TOM20 (Santa Cruz Biotechnology, #sc-11415, 1:1000).

For co-IP analysis, proteins were prepared with non-denaturing lysis buffer and incubated with primary antibodies against HA or isotype control immunoglobulin G (IgG) at 4°C overnight. Then, 50 μl magnetic beads (MCE, #HY-K0205) were added into the mixture and incubated for 4 h with rotation. After removing the surface attachments, samples were obtained from the bead-antibody complexes and subjected to immunoassay as above described. The following antibodies were used in this study: anti-IgG (Proteintech, #30000-0-AP, 1:50) and anti-HA (Proteintech, #51064-2-AP, 1:50).

Immunofluorescence

Cells were fixed with 4% paraformaldehyde for 30 min, permeabilized with 0.1% Triton X-100 for 5 min, and blocked in 5% BSA for 1 h. Then cells were stained with the following primary antibodies overnight at 4°C: Cardiac troponin T (Abcam, #ab8295, 1:200), Samm50 (Proteintech, #28679-1-AP, 1:50), Pink1 (Proteintech, #23274-1-AP, 1:100) and VDAC1 (Santa Cruz Biotechnology, #sc-390996, 1:50). After washing with PBS 3 times, cells were incubated with specific secondary antibodies conjugated to Alexa Fluor for 1 h at 37°C. Five minutes after co-staining with 4',6-diamidino-2-phenylindole (DAPI, Invitrogen, #D1306), the cells were observed by a fluorescence microscope, and cardiomyocyte surface area was calculated by Image-Pro Plus software.

Heart sections were deparaffinized and rehydrated and then antigenically retrieved in sodium citrate buffer for 30 min. The following procedures were conducted according to the protocol described for cardiomyocytes. Co-localization was analyzed by Image-Pro Plus software.

Measurement of Autophagy Flux

Adenovirus harboring tandem fluorescent mRFP-GFP-LC3 system (adenovirus-tf-LC3) was used to evaluate autophagy flux as previously described [28]. Cardiomyocytes plated on coverslips were transfected with adenovirus-tf-LC3 at 10 MOI for 24 h and treated with Ang II for 6 h. Then cells were fixed with 4% paraformaldehyde, stained with DAPI, and observed under a fluorescence microscope. The number of GFP and mRFP dots were recorded by manual counting of fluorescent puncta from at least 50 cells. The number of DAPI-stained nuclei were recorded to represent the nuclear number.

Statistics

All data were presented as mean ± s.e.m. All statistical results were analyzed using GraphPad Prism Software. Statistical analysis of two sets was performed by Student's t-test. Multiple comparisons were conducted by one-way analysis of variance with the Newman–Keuls test. A value of $P < 0.05$ was considered statistically significant.
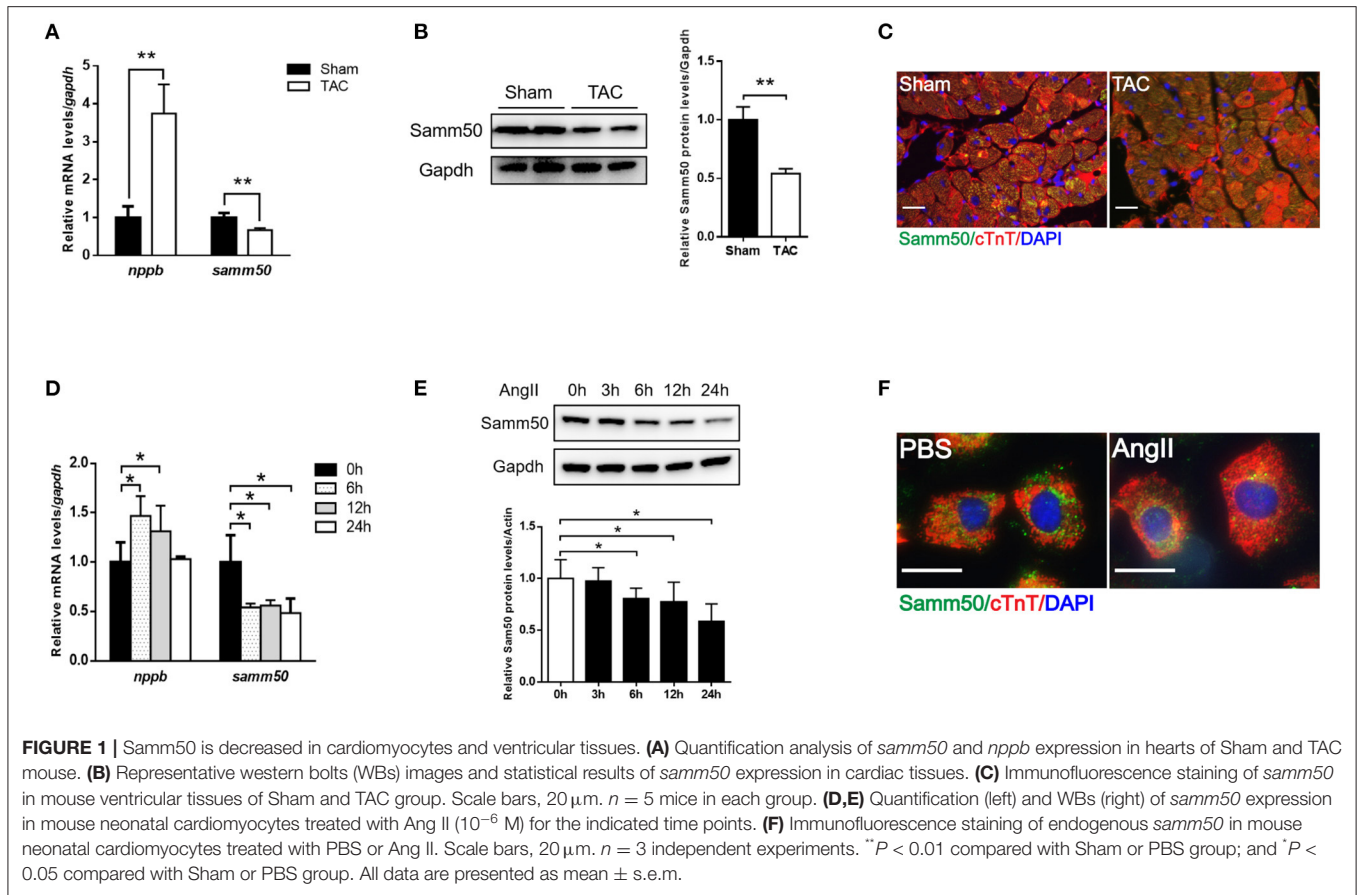
RESULTS

Samm50 Is Downregulated in Myocardial Hypertrophy

To determine whether Samm50 expression is associated with cardiac hypertrophy, we performed the TAC mice model (**Supplementary Figures 1A–D**) and found the mRNA, and protein levels of Samm50 were remarkably decreased in response to pressure overload (**Figures 1A,B**). Parallelly, in the isolated mice neonatal cardiomyocytes, qRT-PCR and western bolt (WB) data showed that Samm50 expression levels were significantly reduced by Ang II stimulation (**Figures 1D,E**). Interestingly, Samm50 expression was unchanged in cardiac fibroblasts under Ang II treatment (**Supplementary Figures 1E,F**). The immunofluorescence staining also showed a consistent result of decreased Samm50 levels in TAC-induced hypertrophic hearts and Ang II-treated cardiomyocytes (**Figures 1C,F**). These results revealed that Samm50 was dramatically downregulated both *in vivo* and *in vitro* in response to hypertrophic stimuli, indicating a potential role of Samm50 in the regulation of cardiac hypertrophy.

Overexpression of Samm50 Exacerbates Cardiomyocyte Hypertrophy and Inhibits Mitophagy

To investigate the potential effect of Samm50 on cardiomyocyte hypertrophy, we transfected lentivirus overexpressed Samm50 into isolated and cultured mice neonatal cardiomyocytes and verified Samm50 expression by WB and qRT-PCR analysis (**Figures 2A,B**). After Ang II administration, the expressions of hypertrophic markers such as *nppb* (natriuretic peptide B), *c-jun* (jun proto-oncogene), *c-fos* (Fos proto-oncogene), and *rcan1.4* (regulator of calcineurin 1, transcript
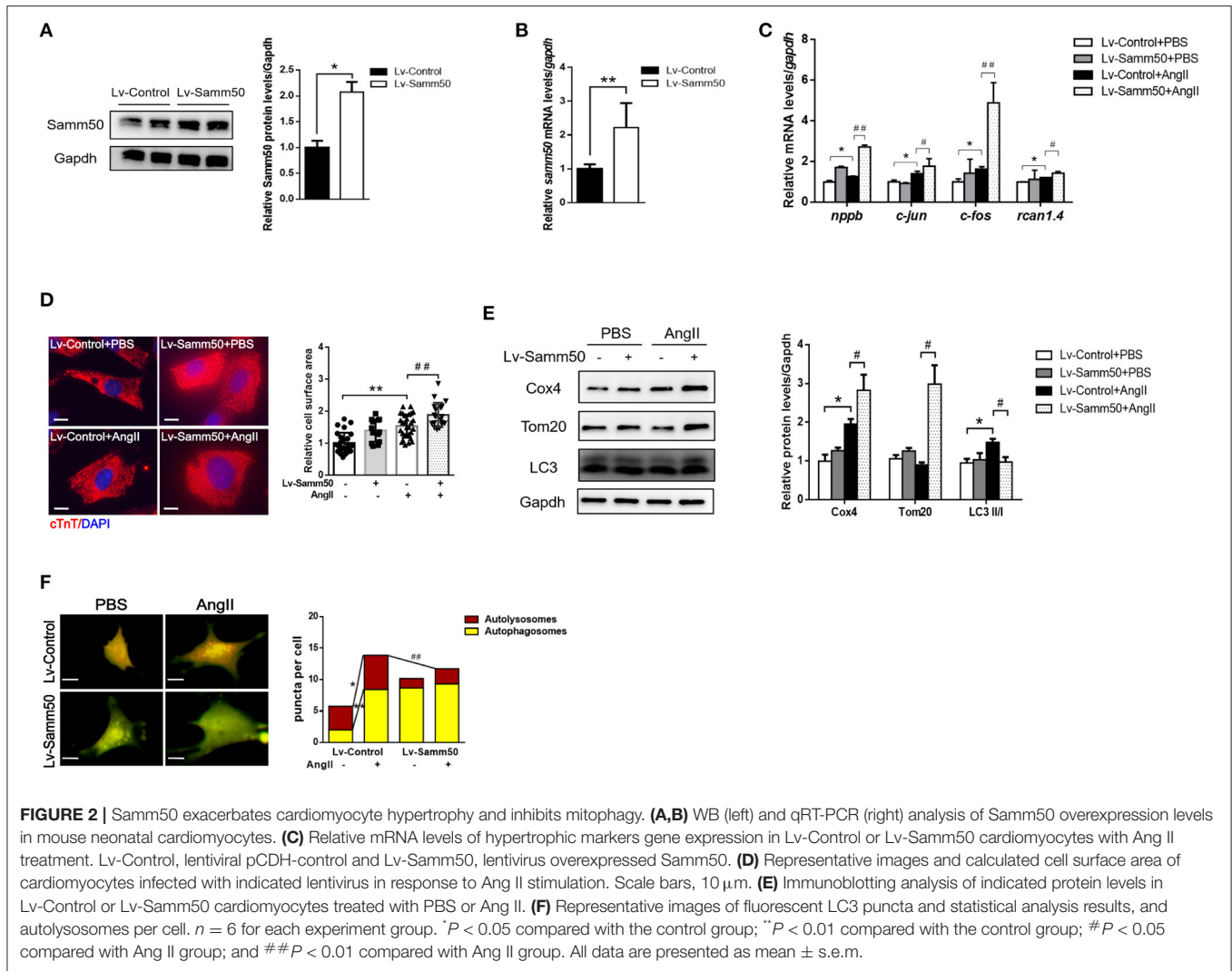
FIGURE 1 | Samm50 is decreased in cardiomyocytes and ventricular tissues. (A) Quantification analysis of *samm50* and *nppb* expression in hearts of Sham and TAC mouse. (B) Representative western bolts (WBs) images and statistical results of *samm50* expression in cardiac tissues. (C) Immunofluorescence staining of *samm50* in mouse ventricular tissues of Sham and TAC group. Scale bars, 20 μm. *n* = 5 mice in each group. (D,E) Quantification (left) and WBs (right) of *samm50* expression in mouse neonatal cardiomyocytes treated with Ang II (10^{-6} M) for the indicated time points. (F) Immunofluorescence staining of endogenous *samm50* in mouse neonatal cardiomyocytes treated with PBS or Ang II. Scale bars, 20 μm. *n* = 3 independent experiments. $**P < 0.01$ compared with Sham or PBS group; and $*P < 0.05$ compared with Sham or PBS group. All data are presented as mean ± s.e.m.

4) were obviously elevated in the Samm50-overexpressed group compared with the control group (**Figure 2C**). Furthermore, cardiomyocytes were incubated with cardiac troponin T to evaluate the cardiomyocyte surface area. As shown in **Figure 2D**, Samm50 overexpression markedly enlarged the cardiomyocyte size in response to Ang II treatment. These data indicated that Samm50 exacerbates cardiac hypertrophy.

Mitochondrial dynamics are critical to maintain cardiomyocyte function, especially under pathological stress. Given that Samm50 is associated with mitochondrial homeostasis and mitophagy (25), we explored whether Samm50 aggravates cardiac hypertrophy by affecting mitochondria function. We first evaluated mitochondrial biogenesis by detecting the expression of mitochondrial *NADH dehydrogenase 1* (*mtND1*). The results showed that *mtND1* was not altered in response to Samm50 overexpression (**Supplementary Figure 1G**). Then, autophagy markers and mitochondria protein levels were assessed by immunoblotting. Compared with the control group, overexpression of Samm50 displayed decreased LC3-II/LC3-I ratio and increased levels of TOM20 and COX4, indicating inhibition of mitophagy in cardiomyocytes (**Figure 2E**). Besides, the adenovirus-tf-LC3 was generated to evaluate autophagic flux. We monitored the number of red and green puncta by fluorescence microscope. The

red puncta overlapped with the green ones are indicators of autophagosomes, while the free red puncta represent autolysosomes (29). As shown in **Figure 2F**, the yellow and red puncta were both increased in Ang II-treated cardiomyocytes, whereas Samm50 overexpression evidently decreased the number of red puncta, and most of them overlaid with the green ones in merged images, indicating Samm50 inhibits autophagic flux. Overall, these data demonstrated that Samm50 exacerbates Ang II-induced cardiomyocyte hypertrophy and inhibits mitophagy.

Samm50 Depletion Attenuates Cardiomyocyte Hypertrophy by Promoting Mitophagy

To further verify the effects of Samm50 on cardiac hypertrophy and heart failure, we performed lentivirus-delivered shRNA to ablate *samm50* expression. The efficacy of *samm50* depletion was confirmed by WB and qRT-PCR analysis, respectively (**Figures 3A,B**). In accordance with the results observed in Samm50 overexpression, Samm50 deficiency remarkably reduced the expression of hypertrophic markers and ameliorated cardiomyocyte size compared with the control group, as evidenced by qRT-PCR and immunofluorescence (**Figures 3C,D**). Knockdown of

FIGURE 2 | Samm50 exacerbates cardiomyocyte hypertrophy and inhibits mitophagy. **(A,B)** WB (left) and qRT-PCR (right) analysis of Samm50 overexpression levels in mouse neonatal cardiomyocytes. **(C)** Relative mRNA levels of hypertrophic markers gene expression in Lv-Control or Lv-Samm50 cardiomyocytes with Ang II treatment. Lv-Control, lentiviral pCDH-control and Lv-Samm50, lentivirus overexpressed Samm50. **(D)** Representative images and calculated cell surface area of cardiomyocytes infected with indicated lentivirus in response to Ang II stimulation. Scale bars, 10 μm. **(E)** Immunoblotting analysis of indicated protein levels in Lv-Control or Lv-Samm50 cardiomyocytes treated with PBS or Ang II. **(F)** Representative images of fluorescent LC3 puncta and statistical analysis results, and autolysosomes per cell. $n = 6$ for each experiment group. $^{*}P < 0.05$ compared with the control group; $^{**}P < 0.01$ compared with the control group; $^{\#}P < 0.05$ compared with Ang II group; and $^{\#\#}P < 0.01$ compared with Ang II group. All data are presented as mean ± s.e.m.
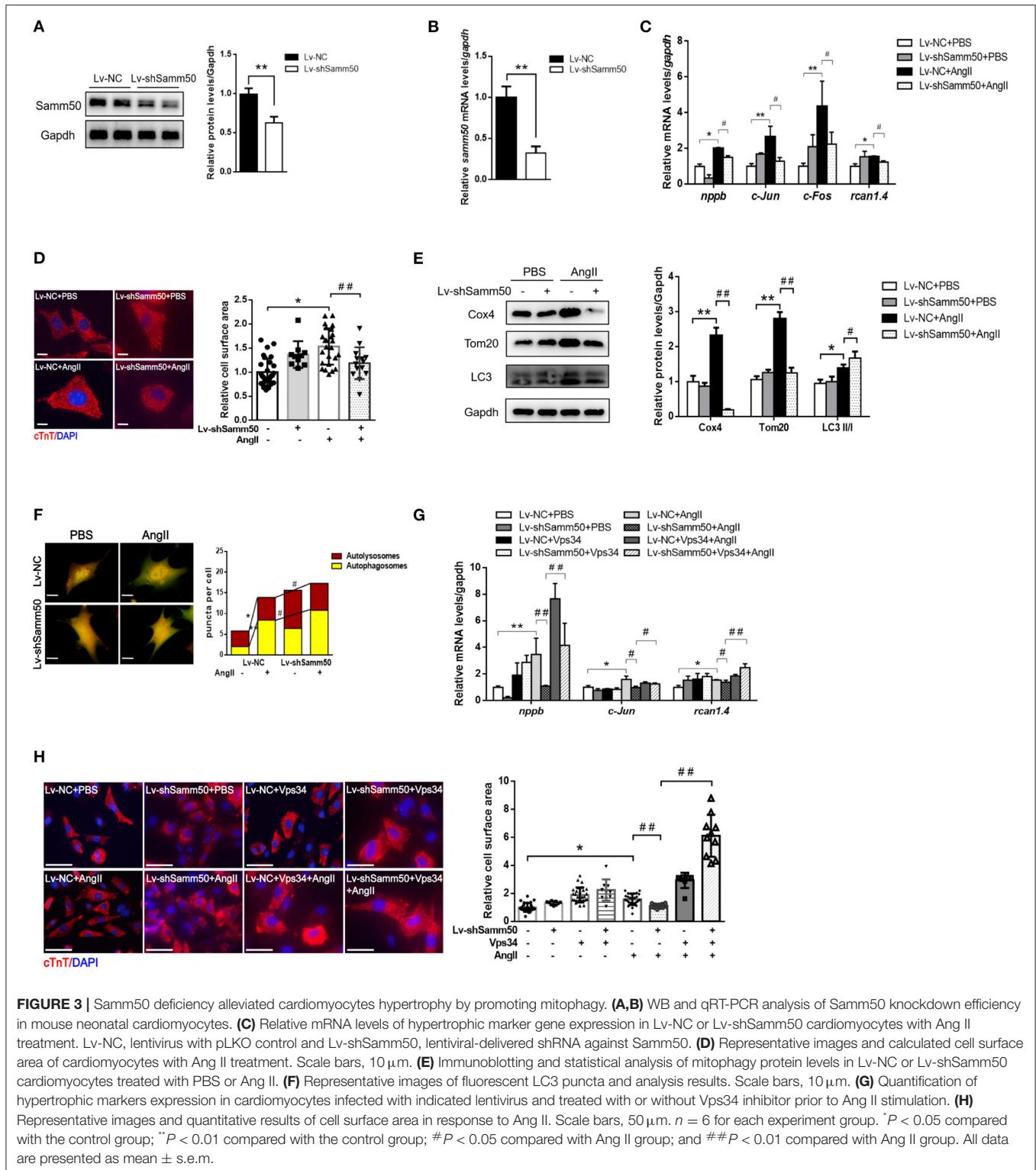
Samm50 also exhibited increased mitophagy, manifested by an increase in LC3-II/LC3-I ratio and a decrease in TOM20 and COX4. Furthermore, in response to Ang II treatment, Samm50 ablation caused a significant accumulation of red puncta, which was greater than that in yellow puncta, indicating Samm50 increases autophagosomes more than autophagosomes and thus stimulates autophagic flux (**Figure 3F**). These results suggested that Samm50 deficiency ameliorates cardiomyocyte hypertrophy and enhanced mitophagy.

To evaluate the role of mitophagy in Samm50-mediated cardiac hypertrophy, we introduced an autophagy inhibitor into the Samm50-depleted cardiomyocyte prior to Ang II stimulation. Notably, the protective effect of Samm50-deficiency on cardiomyocyte hypertrophy was largely diminished in the presence of autophagy inhibitors, as demonstrated by the increases of hypertrophic markers and cardiomyocyte size (**Figures 3G,H**), further supporting the idea that mitophagy is required for Samm50-mediated cardiomyocyte hypertrophy.

Samm50 Regulates Pink1-Parkin-Mediated Mitophagy in Myocardial Hypertrophy

The previous study has suggested that Samm50-mediated mitophagy is dependent on the Pink1-Parkin pathway under cancer conditions (25). To further elucidate the underlying mechanism of Samm50 in the regulation of myocardial hypertrophy, we first detected the expression of Pink1 and Parkin in response to Ang II stimulation. As seen in **Figure 4A**, knockdown of Samm50 caused accumulation of Pink1 and Parkin, indicating the activation of mitophagy in cardiomyocytes. However, Pink1 and Parkin expression had no obvious difference between Samm50 overexpression and control group (**Figure 4B**). To evaluate whether Pink1 is required for Samm50-mediated cardiac hypertrophy, we interfered with the expression of Pink1 in the absence of Samm50. Our data revealed that Samm50 depletion-trigged activation of mitophagy was blunted in cardiomyocytes with simultaneous Pink1 knockout, as indicated by decreased LC3-II/LC3-I ratio and increased protein level of TOM20 and COX4 (**Figure 4C**). Consistent

FIGURE 3 | Samm50 deficiency alleviated cardiomyocytes hypertrophy by promoting mitophagy. **(A,B)** WB and qRT-PCR analysis of Samm50 knockdown efficiency in mouse neonatal cardiomyocytes. **(C)** Relative mRNA levels of hypertrophic marker gene expression in Lv-NC or Lv-shSamm50 cardiomyocytes with Ang II treatment. Lv-NC, lentivirus with pLKO control and Lv-shSamm50, lentiviral-delivered shRNA against Samm50. **(D)** Representative images and calculated cell surface area of cardiomyocytes with Ang II treatment. Scale bars, 10 μm. **(E)** Immunoblotting and statistical analysis of mitophagy protein levels in Lv-NC or Lv-shSamm50 cardiomyocytes treated with PBS or Ang II. **(F)** Representative images of fluorescent LC3 puncta and analysis results. Scale bars, 10 μm. **(G)** Quantification of hypertrophic markers expression in cardiomyocytes infected with indicated lentivirus and treated with or without Vps34 inhibitor prior to Ang II stimulation. **(H)** Representative images and quantitative results of cell surface area in response to Ang II. Scale bars, 50 μm. $n = 6$ for each experiment group. $^{*}P < 0.05$ compared with the control group; $^{**}P < 0.01$ compared with the control group; $^{\#}P < 0.05$ compared with Ang II group; and $^{\#\#}P < 0.01$ compared with Ang II group. All data are presented as mean ± s.e.m.

with immunoblotting results, the protective effect of Samm50 deficiency in response to Ang II induction was blocked by Pink1 knockdown, which was manifested by enhanced hypertrophic markers and cardiomyocyte enlargement (**Figures 4D,E**).

Based on Samm50 interaction with Pink1 and regulation of its stability (25), we transfected HL-1 cells with HA-tagged Samm50 and Flag-tagged Pink1, followed by Ang II treatment and co-IP analysis to explore whether their physical interaction changes
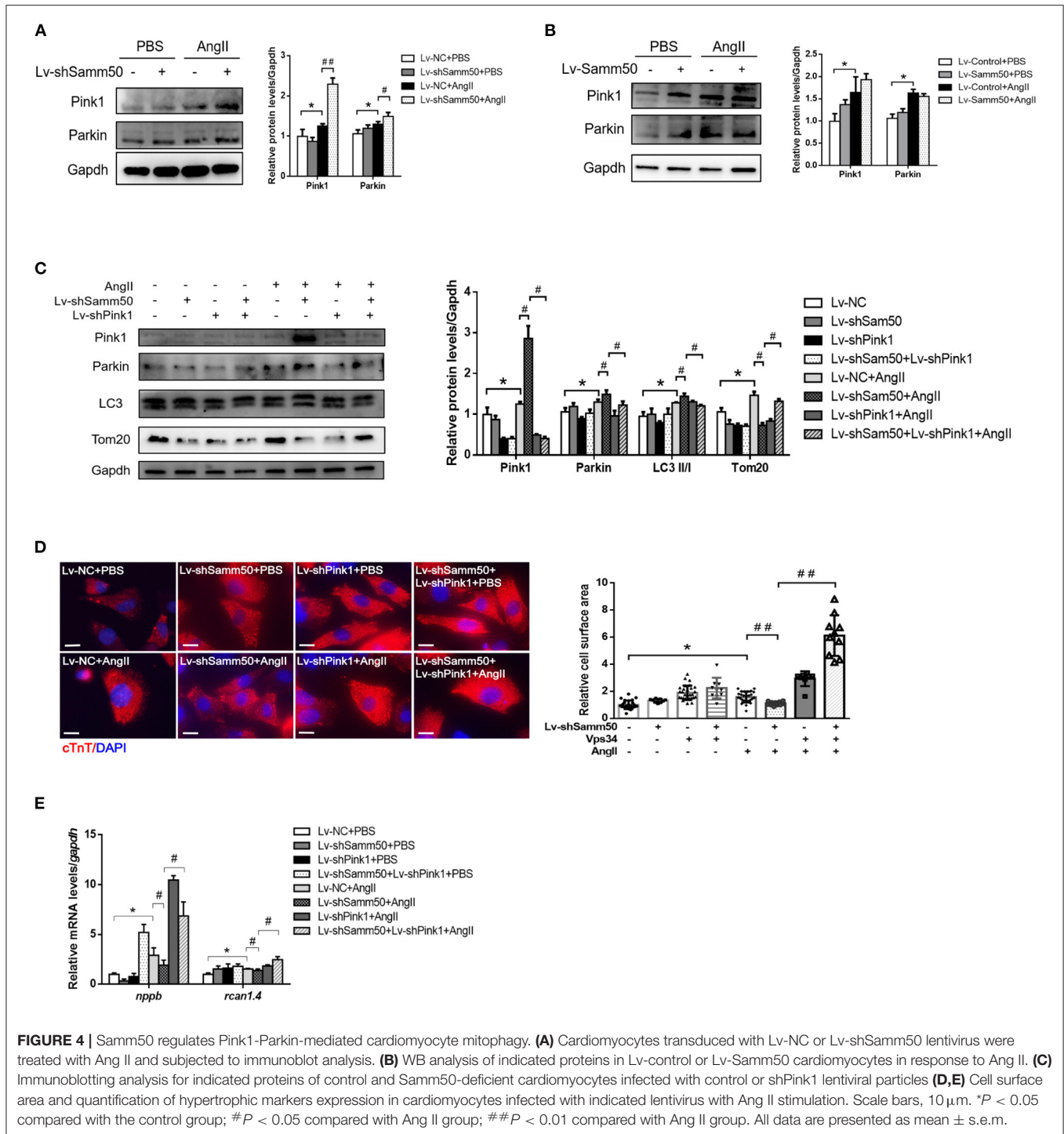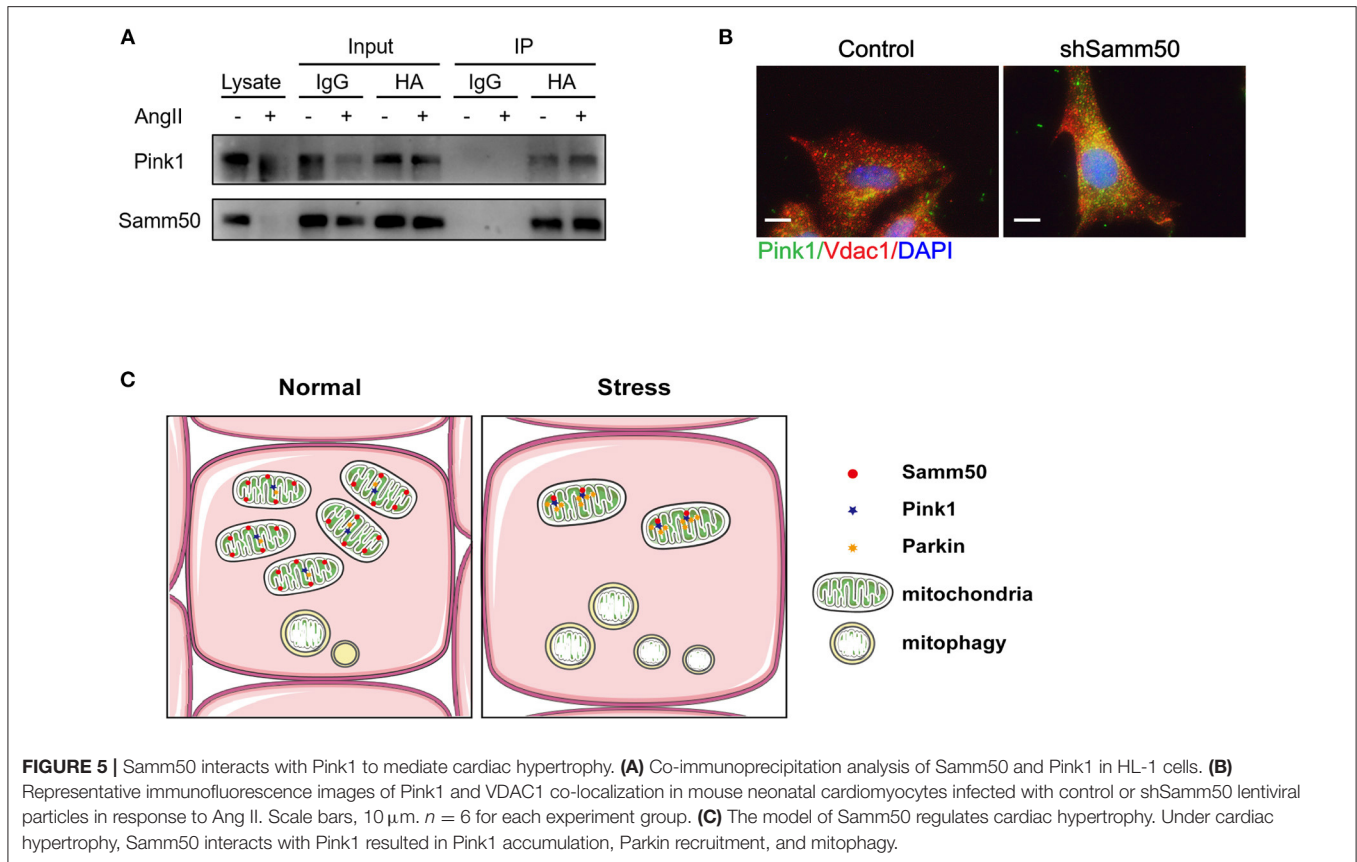
FIGURE 4 | Samm50 regulates Pink1-Parkin-mediated cardiomyocyte mitophagy. **(A)** Cardiomyocytes transduced with Lv-NC or Lv-shSamm50 lentivirus were treated with Ang II and subjected to immunoblot analysis. **(B)** WB analysis of indicated proteins in Lv-control or Lv-Samm50 cardiomyocytes in response to Ang II. **(C)** Immunoblotting analysis for indicated proteins of control and Samm50-deficient cardiomyocytes infected with control or shPink1 lentiviral particles **(D,E)** Cell surface area and quantification of hypertrophic markers expression in cardiomyocytes infected with indicated lentivirus with Ang II stimulation. Scale bars, 10 μm. *$P < 0.05$ compared with the control group; #$P < 0.05$ compared with Ang II group; ##$P < 0.01$ compared with Ang II group. All data are presented as mean ± s.e.m.

under Ang II stimulation. The co-IP of Samm50 by HA antibody exhibited an interaction between Samm50 and Pink1 in HL-1 cells, while there was no significant difference in the level of Pink1 detected in the absence or presence of Ang II, indicating the interaction between Samm50 and Pink1 was not influenced by Ang II stimulation (**Figure 5A**).

Pink1 and Parkin were recruited during mitophagy and accumulated in mitochondria (16). To further verify the activation of the Pink1/Parkin pathway in Samm50-mediated hypertrophy, we utilized the immunofluorescent staining to visualize the subcellular localization of Parkin and mitochondria in Samm50-deficient cardiomyocytes. The results showed

FIGURE 5 | Samm50 interacts with Pink1 to mediate cardiac hypertrophy. **(A)** Co-immunoprecipitation analysis of Samm50 and Pink1 in HL-1 cells. **(B)** Representative immunofluorescence images of Pink1 and VDAC1 co-localization in mouse neonatal cardiomyocytes infected with control or shSamm50 lentiviral particles in response to Ang II. Scale bars, 10 μm. $n = 6$ for each experiment group. **(C)** The model of Samm50 regulates cardiac hypertrophy. Under cardiac hypertrophy, Samm50 interacts with Pink1 resulted in Pink1 accumulation, Parkin recruitment, and mitophagy.

that Parkin was predominantly stained with mitochondria marker VDAC1 (**Figure 5B**), indicating the accumulation of Parkin in mitochondria. Overall, these results demonstrate that Samm50 regulates cardiomyocyte hypertrophy in a Pink1/Parkin-dependent manner.

DISCUSSION

Cardiac hypertrophy is one of the primary reasons for heart failure. Pathological gene reprogramming could develop cardiac hypertrophy. This process is governed by multiple factors that could coordinate cardiac remodeling or against remodeling. Here, we identified a member of mitochondrial SAM complex, Samm50, which positively regulates cardiac hypertrophy involving mitophagy. We first observed the downregulation of Samm50 expression in the TAC model and Ang II-treated cardiomyocytes. Using gain- and loss-of-function approaches, we determined the potential role of Samm50 on pathological cardiac hypertrophy. Our results showed that Samm50 exacerbates cardiac hypertrophy by inhibiting mitophagy.

The more recent development of signaling effectors of cardiac hypertrophy is identified using genetically modified mouse models and primary cardiomyocytes. Mechanical stress, humoral stimuli, chromatin remodeling, inflammation, redox,

and Ca^{2+} signaling were discovered to be strongly involved in cardiac hypertrophy (30). Furthermore, mitochondrial dysfunction has been indicated as a potential and important player in the development of cardiac hypertrophy (31). Mitophagy is essential to mitochondria homeostasis. However, few studies focus on the relationship between mitophagy and cardiac hypertrophy. One study showed that macrophage migration inhibitory factor significantly reduced pressure overload-induced cardiac hypertrophy by activating mitophagy and autophagy (32). Another one showed that the knockdown of lysocardiolipin acyltransferase 1 upregulates mitophagy to mitigate cardiac dysfunction associated with cardiac hypertrophy (33). Given that Samm50 was reported as a regulator of mitophagy and mitochondrial function, we first explored the involvements of mitochondria biogenesis in Samm50-mediated cardiomyocyte hypertrophy. Consistent with the previous study, the mitochondrial DNA copy number was not altered in these groups (**Supplementary Figure 1G**). We further observed that Samm50 depletion attenuates cardiomyocyte hypertrophy and promotes mitophagy (**Figures 3C–F**), indicating that Samm50 might inhibit mitophagy to exacerbate cardiac hypertrophy. Thus, we investigated the effect of autophagy inhibitors on the effect of Samm50 depletion in response to Ang II. The results revealed that the Vps34 inhibitor largely diminished the protective effect of Samm50 deficiency on Ang II-induced hypertrophy (**Figures 3G,H**), indicating the

beneficial function of mitophagy in cardiac hypertrophy and that Samm50 regulates cardiomyocyte hypertrophy by inhibiting mitophagy. This result enlarged our understanding of mitophagy in cardiac hypertrophy.

Cardiac hypertrophy decompensation could be regulated by mitochondrial reprogramming. Samm50 is widely known as an essential protein of the mitochondrial outer membrane and has been verified to interact directly with the TOM complex to facilitate the biogenesis of ß-barrel protein. However, whether Samm50 participates in the cardiac hypertrophy process remains unclear. In our study, we found that the expression of Samm50 was significantly downregulated *in vivo* and *in vitro* cardiac hypertrophy model (**Figures 1A–F**), indicating that the changes of Samm50 maybe play a role in cardiac hypertrophy. To further clarify the relationship between Samm50 and hypertrophy, we conducted gain- and loss-of-function studies using lentivirus. We found that Samm50 overexpression aggravated the expression of hypertrophic markers and enlarged the cardiomyocyte size in response to Ang II (**Figures 2C,D**). Meanwhile, knockdown Samm50 could ameliorate cardiac hypertrophy (**Figures 3C,D**). Further understanding the mechanism by which Samm50 regulates mitophagy in cardiac hypertrophy is important for exploring the new strategies for treatment. Samm50 is a critical regulator of Pink1-Parkin-mediated or P62-mediated mitophagy (25, 34), whereas most mitophagy signals converge on the Pink1-Parkin-mediated pathway. Fenglei et al. revealed that Samm50 interacts with Pink1 and regulates its stability in HeLa cells (25). Agreed with the previous study, our results showed that Samm50 could directly interact with Pink1 in the cardiac hypertrophy model (**Figure 5A**). Besides, interference with Pink1 can eliminate the activation of mitophagy and the protective effect induced by Samm50 deficiency (**Figures 4D,E**). Collectively, we first discovered that Samm50-mediated mitophagy in cardiac hypertrophy was largely dependent on Pink1-Parkin signaling (**Figure 5C**). However, further experiments need to be performed to elaborate the mechanism involved in modulating Pink-Parkin by Samm50.

In conclusion, our present study shows Samm50 aggravates cardiac hypertrophy by regulating the Pink1-Parkin signaling and further clarifies the relationship between mitophagy and cardiac hypertrophy. These results may provide new insights into the treatment of cardiac hypertrophy.

DATA AVAILABILITY STATEMENT

The raw data supporting the conclusions of this article will be made available by the authors, without undue reservation.

ETHICS STATEMENT

The animal study was reviewed and approved by the Animal Care and Use Committee of Zhongshan Hospital, Fudan University.

AUTHOR CONTRIBUTIONS

FUNDING

SUPPLEMENTARY MATERIAL

The Supplementary Material for this article can be found online at: https://www.frontiersin.org/articles/10.3389/fcvm.2021.748156/full#supplementary-material

REFERENCES

1. Oldfield CJ, Duhamel TA, Dhalla NS. Mechanisms for the transition from physiological to pathological cardiac hypertrophy. *Can J Physiol Pharmacol.* (2020) 98:74–84. doi: 10.1139/cjpp-2019-0566
2. Nakamura M, Sadoshima J. Mechanisms of physiological and pathological cardiac hypertrophy. *Nat Rev Cardiol.* (2018) 15:387–407. doi: 10.1038/s41569-018-0007-y
3. Wu J, You J, Wang X, Wang S, Huang J, Xie Q, et al. Left ventricular response in the transition from hypertrophy to failure recapitulates distinct roles of Akt, β-arrestin-2, and CaMKII in mice with aortic regurgitation. *Ann Transl Med.* (2020) 8:219. doi: 10.21037/atm.2020.01.51
4. Mutlak M, Kehat I. Extracellular signal-regulated kinases 1/2 as regulators of cardiac hypertrophy. *Front Pharmacol.* (2015) 6:149. doi: 10.3389/fphar.2015.00149
5. Miao R, Lu Y, Xing X, Li Y, Huang Z, Zhong H, et al. Regulator of G-protein signaling 10 negatively regulates cardiac remodeling by blocking mitogen-activated protein kinase-extracellular signal-regulated protein kinase 1/2 signaling. *Hypertension.* (2016) 67:86–98. doi: 10.1161/HYPERTENSIONAHA.115.05957

6. Heineke J, Molkentin JD. Regulation of cardiac hypertrophy by intracellular signalling pathways. *Nat Rev Mol Cell Biol.* (2006) 7:589–600. doi: 10.1038/nrm1983
7. Gibb AA, Hill BG. Metabolic coordination of physiological and pathological cardiac remodeling. *Circ Res.* (2018) 123:107–28. doi: 10.1161/CIRCRESAHA.118.312017
8. Ding Z, Yuan J, Liang Y, Wu J, Gong H, Ye Y, et al. Ryanodine receptor type 2 plays a role in the development of cardiac fibrosis under mechanical stretch through TGFβ-1. *Int Heart J.* (2017) 58:957–61. doi: 10.1536/ihj.16-572
9. Nakai A, Yamaguchi O, Takeda T, Higuchi Y, Hikoso S, Taniike M, et al. The role of autophagy in cardiomyocytes in the basal state and in response to hemodynamic stress. *Nat Med.* (2007) 13:619–24. doi: 10.1038/nm1574
10. Kuzman JA, O'Connell TD, Gerdes AM. Rapamycin prevents thyroid hormone-induced cardiac hypertrophy. *Endocrinology.* (2007) 148:3477–84. doi: 10.1210/en.2007-0099
11. Ha T, Li Y, Gao X, McMullen JR, Shioi T, Izumo S, et al. Attenuation of cardiac hypertrophy by inhibiting both mTOR and NFkappaB activation *in vivo*. *Free Radic Biol Med.* (2005) 39:1570–80. doi: 10.1016/j.freeradbiomed.2005.08.002
12. Aguirre S, Luthra P, Sanchez-Aparicio MT, Maestre AM, Patel J, Lamothe F, et al. Dengue virus NS2B protein targets cGAS for degradation and

prevents mitochondrial DNA sensing during infection. *Nat Microbiol.* (2017) 2:17037. doi: 10.1038/nmicrobiol.2017.37

13. Harper JW, Ordureau A, Heo JM. Building and decoding ubiquitin chains for mitophagy. *Nat Rev Mol Cell Biol.* (2018) 19:93–108. doi: 10.1038/nrm.2017.129

14. Koyano F, Okatsu K, Kosako H, Tamura Y, Go E, Kimura M, et al. Ubiquitin is phosphorylated by PINK1 to activate parkin. *Nature.* (2014) 510:162–6. doi: 10.1038/nature13392

15. Lazarou M, Jin SM, Kane LA, Youle RJ. Role of PINK1 binding to the TOM complex and alternate intracellular membranes in recruitment and activation of the E3 ligase Parkin. *Dev Cell.* (2012) 22:320–33. doi: 10.1016/j.devcel.2011.12.014

16. Lazarou M, Sliter DA, Kane LA, Sarraf SA, Wang C, Burman JL, et al. The ubiquitin kinase PINK1 recruits autophagy receptors to induce mitophagy. *Nature.* (2015) 524:309–14. doi: 10.1038/nature14893

17. Pickles S, Vigié P, Youle RJ. Mitophagy and quality control mechanisms in mitochondrial maintenance. *Curr Biol.* (2018) 28:R170–85. doi: 10.1016/j.cub.2018.01.004

18. Sekine S, Youle RJ. PINK1 import regulation; a fine system to convey mitochondrial stress to the cytosol. *BMC Biol.* (2018) 16:2. doi: 10.1186/s12915-017-0470-7

19. Wiedemann N, Kozjak V, Chacinska A, Schönfisch B, Rospert S, Ryan MT, et al. Machinery for protein sorting and assembly in the mitochondrial outer membrane. *Nature.* (2003) 424:565–71. doi: 10.1038/nature01753

20. Qiu J, Wenz LS, Zerbes RM, Oeljeklaus S, Bohnert M, Stroud DA, et al. Coupling of mitochondrial import and export translocases by receptor-mediated supercomplex formation. *Cell.* (2013) 154:596–608. doi: 10.1016/j.cell.2013.06.033

21. Kozjak V, Wiedemann N, Milenkovic D, Lohaus C, Meyer HE, Guiard B, et al. An essential role of Sam50 in the protein sorting and assembly machinery of the mitochondrial outer membrane. *J Biol Chem.* (2003) 278:48520–3. doi: 10.1074/jbc.C300442200

22. Ding C, Wu Z, Huang L, Wang Y, Xue J, Chen S, et al. Mitofilin and CHCHD6 physically interact with Sam50 to sustain cristae structure. *Sci Rep.* (2015) 5:16064. doi: 10.1038/srep16064

23. Ott C, Ross K, Straub S, Thiede B, Götz M, Goosmann C, et al. Sam50 functions in mitochondrial intermembrane space bridging and biogenesis of respiratory complexes. *Mol Cell Biol.* (2012) 32:1173–88. doi: 10.1128/MCB.06388-11

24. Liu S, Gao Y, Zhang C, Li H, Pan S, Wang X, et al. SAMM50 affects mitochondrial morphology through the association of drp1 in mammalian cells. *FEBS Lett.* (2016) 590:1313–23. doi: 10.1002/1873-3468.12170

25. Jian F, Chen D, Chen L, Yan C, Lu B, Zhu Y, et al. Sam50 regulates PINK1-parkin-mediated mitophagy by controlling PINK1 stability and mitochondrial morphology. *Cell Rep.* (2018) 23:2989–3005. doi: 10.1016/j.celrep.2018.05.015

26. Hu Z, Ding X, Ji Y, Liu X, Ding Z. APEX1 protects against oxidative damage-induced cardiomyocyte apoptosis.

Biocell. (2021) 45:745–9. doi: 10.32604/biocell.2021.013293

27. Livak KJ, Schmittgen TD. Analysis of relative gene expression data using real-time quantitative PCR and the 2(-Delta Delta C(T)) Method. *Methods.* (2001) 25:402–8. doi: 10.1006/meth.2001.1262

28. Hariharan N, Zhai P, Sadoshima J. Oxidative stress stimulates autophagic flux during ischemia/reperfusion. *Antioxid Redox Signal.* (2011) 14:2179–90. doi: 10.1089/ars.2010.3488

29. Kimura S, Noda T, Yoshimori T. Dissection of the autophagosome maturation process by a novel reporter protein, tandem fluorescent-tagged LC3. *Autophagy.* (2007) 3:452–60. doi: 10.4161/auto.4451

30. Samak M, Fatullayev J, Sabashnikov A, Zeriouh M, Schmack B, Farag M, et al. Cardiac Hypertrophy: An Introduction to Molecular and Cellular Basis. *Med Sci Monit Basic Res.* (2016) 22:75–9. doi: 10.12659/MSMBR.900437

31. Vásquez-Trincado C, García-Carvajal I, Pennanen C, Parra V, Hill JA, Rothermel BA, et al. Mitochondrial dynamics, mitophagy and cardiovascular disease. *J Physiol.* (2016) 594:509–25. doi: 10.1113/JP271301

32. Xu X, Hua Y, Nair S, Bucala R, Ren J. Macrophage migration inhibitory factor deletion exacerbates pressure overload-induced cardiac hypertrophy through mitigating autophagy. *Hypertension.* (2014) 63:490–9. doi: 10.1161/HYPERTENSIONAHA.113.02219

33. Liu X, Ye B, Miller S, Yuan H, Zhang H, Tian L, et al. Ablation of ALCAT1 mitigates hypertrophic cardiomyopathy through effects on oxidative stress and mitophagy. *Mol Cell Biol.* (2012) 32:4493–504. doi: 10.1128/MCB.01092-12

34. Abudu YP, Shrestha BK, Zhang W, Palara A, Brenne HB, Larsen KB, et al. SAMM50 acts with p62 in piecemeal basal- and OXPHOS-induced mitophagy of SAM and MICOS components. *J Cell Biol.* (2021) 220:e202009092. doi: 10.1083/jcb.202009092